1 *Article*

2 # Introduction of an experimental terrestrial
3 # forecasting/monitoring system at regional to
4 # continental scales based on the Terrestrial System
5 # Modeling Platform (v1.1.0)

6 **Stefan Kollet[1,2,*], Fabian Gasper[1,2,**], Slavko Brdar[3,2], Klaus Goergen[1,2], Harrie-Jan**
7 **Hendricks-Franssen[1,2], Jessica Keune[1,4,2,***], Wolfgang Kurtz[1,2,****], Volker Küll[4], Florian**
8 **Pappenberger[5], Stefan Poll[4], Silke Trömel[4], Prabhakar Shrestha[4], Clemens Simmer[4,2], and Mauro**
9 **Sulis[4,*****]**

10 [1] Agrosphere Inst., IBG-3, Inst. of Bio-Geosciences, Forschungszentrum Jülich GmbH, Jülich, Germany
11 [2] Centre for High-Performance Scientific Computing, Geoverbund ABC/J, Germany
12 [3] Jülich Supercomputing Centre, Forschungszentrum Jülich GmbH, Jülich, Germany
13 [4] Meteorological Institute, Bonn University, Germany
14 [5] European Centre for Medium-Range Weather Forecasts
15 * Correspondence: s.kollet@fz-juelich.de; Tel.: +49-2461-61-9593
16 ** Now at CISS TDI GmbH, Sinzig, Germany
17 *** Now at the Department of Environment, Ghent University, Belgium
18 **** Now at Environmental Computing Group, Leibniz Supercomputing Centre, Germany
19 ***** Now at the Department of Environmental Research and Innovation, Luxembourg Institute of Science
20 and Technology, Luxembourg

21

22 **Abstract:** Operational weather and also flood forecasting has been performed successfully for
23 decades and is of great socioeconomic importance. Up to now, forecast products focus on
24 atmospheric variables, such as precipitation, air temperature and, in hydrology, on river discharge.
25 Considering the full terrestrial system from groundwater across the land surface into the
26 atmosphere, a number of important hydrologic variables are missing especially with regard to the
27 shallow and deeper subsurface (e.g. groundwater), which are gaining considerable attention in the
28 context of global change. In this study, we propose a terrestrial monitoring/forecasting system
29 using the Terrestrial Systems Modeling Platform (TSMP) that predicts all essential states and fluxes
30 of the terrestrial hydrologic and energy cycles from groundwater into the atmosphere. Closure of
31 the terrestrial cycles provides a physically consistent picture of the terrestrial system in TSMP.
32 TSMP has been implemented over a regional domain over North Rhine-Westphalia and a
33 continental domain over Europe in a real-time forecast/monitoring workflow. Applying a real-time
34 forecasting/monitoring workflow over both domains, experimental forecasts are being produced
35 with different lead times since the beginning of 2016. Real-time forecast/monitoring products
36 encompass all compartments of the terrestrial system including additional hydrologic variables,
37 such as plant available soil water, groundwater table depth, and groundwater recharge and
38 storage.

39 **Keywords:** terrestrial modeling; real-time forecasting/monitoring; workflows

40

41 ## 1. Introduction

42 Weather forecasting operates at global and local scale providing predictions into the future
43 from minutes, hours, and days to months on spatial scales from 100 meters to several kilometers [1].

44   Most national weather services such as e.g. the German national weather service DWD (Deutscher
45   Wetterdienst) [2] and the European Centre for Medium-Range Weather Forecasts [3] develop and
46   operate such forecasting systems. Weather forecasting systems constitute a major infrastructure
47   consisting of state-of-the-art software stacks and supercomputing hardware technologies, real-time
48   data streams of in-situ and remotely sensed observations, and global data exchange infrastructures
49   [4]. In operational forecasting, the software stack consists of a number of sophisticated components
50   including pre- and post-processing tools, the numerical weather prediction (NWP) model, and data
51   assimilation (DA) software, which constitute the kernel of the prediction system and comprise
52   decades of natural science findings and scientific software design knowledge (e.g. [3], [5-7]). In
53   essence, these prediction systems provide real-time forecasts of the states and fluxes in the
54   atmosphere based on a set of initial conditions and, in the case of regional forecasts, lateral boundary
55   conditions, which are continuously corrected with observations through data assimilation. In many
56   atmospheric centers, the software stacks are implemented on some of the most powerful parallel
57   computing and storage hardware available today providing the required capacity and redundancy.
58   Therefore, in terms of operational forecasting, the national weather services represent the
59   state-of-the-art [5]. In addition, there exists a large number of post-processed products of available
60   institutional numerical weather prediction simulation results, so-called re-analyses.

61   Similarly, in hydrologic forecasting of flood events, numerical hydrologic ensemble prediction
62   systems (HEPSs) are paired with DA technologies in operational forecasting frameworks similar to
63   NWP systems briefly outlined above [8-11]. A number of HEPS exist around the world (see for
64   example, EFAS, the European Flood Alert System center [9] and the NOAA National Water Model in
65   the US). In the hydrologic forecast realm, agricultural drought prediction receives attention and
66   poses a number of additional scientific and applied challenges, because of long-term memory effects
67   in the physical processes and scarcity of observations [12]. Often, drought information is made
68   available in so-called drought monitors, which provide recent hindsight information
69   (http://droughtmonitor.unl.edu/) based on input from NWP and atmospheric reanalysis products. It
70   is important that drought forecasts extend further into the vadose zone and groundwater because
71   these compartments constitute essential water storages relevant for e.g. public water supply,
72   agriculture and industry. While water resources management is considered a hot topic worldwide,
73   only very few operational, real-time water resources prediction system are implemented in an
74   institutionalized fashion online today. Examples include The Netherlands Hydrologic Instrument
75   [13] and the US National Water Model, which however does not include the groundwater
76   compartment and focuses on stream discharge and land surface variables (http://water.noaa.gov/).

77   In summary, juxtaposing NWP and HEPS, we note that while there is a plethora of literature on
78   even real-time HEPSs in the scientific community, the large majority of HEPS developments and
79   applications remain in the scientific realm and have not been operationalized. Moreover, NWP and
80   HEPS compartmentalize the earth system into the atmosphere and land surface-soil domains instead
81   of providing a complete and physically consistent forecast of the water, energy and momentum
82   cycles from the bedrock to the top of the atmosphere. In addition, the groundwater compartment is
83   generally missing in the simulations. The situation is, of course, rooted in the complexity and
84   sometimes limited understanding of the system, the lack of adequate computing resources, the
85   objectives of the specific forecast, and legislative mandates.

86   As a result, consistent forecasts of the complete terrestrial water and energy cycle from
87   groundwater across the land surface into the atmosphere at scientific and socioeconomic relevant
88   space and time scales are missing. This also holds for the current state of water resources, which is
89   generally only known from sparse, local in-situ observations and temporal snapshots from remote
90   sensing of the land surface. Thus, society is exposed to a large degree of uncertainty with respect to
91   the current and future state of freshwater resources, the future trajectory of water use and
92   management, and water related hazards, such as floods and droughts.

93   In this paper, we present an implementation of a fully automatized, regional to continental scale
94   forecasting/monitoring system from groundwater into the atmosphere based on the Terrestrial
95   Systems Modeling Platform, TSMP [14, 15]. The overarching goal of the system is to extend the

96   atmospheric-centric view of forecasting to the complete terrestrial ecohydrological system
97   ultimately including the biosphere. TSMP, developed within the framework of the Transregional
98   Collaborative Research Centre TR32 [16] has been applied in a wide variety of studies ranging from
99   the regional to the continental scale with generally reasonable agreement to observations [17-21]. In
100 addition, human water use has been implemented also assessing the potential added value in the
101 comparison to precipitation and evapotranspiration products [22, 23].
102   In this study, the term monitoring system is preferred, in order to emphasize the reciprocity of
103 model based simulations and observations in the application of data assimilation technologies:
104 Models are used to interpolate (in space and time) between observations providing information
105 everywhere and at any time, while observations are used to correct the simulations acknowledging
106 model and observational uncertainties. Currently, the monitoring system produces time lapse
107 images of all relevant states and fluxes of the terrestrial water and energy cycle (table 1) at the
108 applied model resolution including uncertainty estimates. The system is considered as a blueprint of
109 an operational system ultimately merging all available observations from the subsurface to the
110 atmosphere with a physics-based, high-resolution terrestrial model to provide best estimates of the
111 current state of the system and to generate forecasts/projections at resolutions relevant for scientists
112 and stakeholders. Here, we highlight technical requirements, the experimental design, and
113 considerations on improving prediction accuracy with precipitation radar integration as preliminary
114 steps to data assimilation. Validation of the simulation results will be subject of a future study
115 honoring the coupling of all variables of the terrestrial water and energy cycle, and including
116 observation uncertainty. New approaches must be developed to account for mass and energy
117 closure from groundwater into the atmosphere. In the following, we outline and describe the
118 components of the monitoring system, provide information on the workflow and details of the
119 automaion, example forecast products, and a discussion of the path forward.
120
121   Table 1. Selected essential states and fluxes simulated by the terrestrial monitoring system.

Variable name	Units
Subsurface hydraulic pressure	[m]
Subsurface relative saturation	[-]
Subsurface Darcy flow	[mh^{-1}]
Overland flow, surface runoff	[ms^{-1}]
Evaportranspiration	[mms^{-1}] or [Wm^{-2}]
Sensible heat	[Wm^{-2}]
Ground heat	[Wm^{-2}]
Long/short wave radiation (incoming and outgoing)	[Wm^{-2}]
Precipitation (liquid and frozen)	[mms^{-1}]
Snow water equivalent	[m]
Barometric pressure	[Pa]
Air temperature	[K]
Air humidity	[kgkg^{-1}]
Air wind speeds	[ms^{-1}]
Cloud cover	[-]

122

2. Materials and Methods: Terrestrial Monitoring System's components and domains

The kernel of the Terrestrial Monitoring System (TMS) consists of a number of simulation software and hardware components, and data streams, which are linked in a scripted, automated workflow (Section 3). The software components encompass the actual forward or forecast model TSMP (Terrestrial Systems Modeling Platform), which has been proposed by [14] and installed at a Linux cluster of the Jülich Supercomputing Centre. TSMP has been implemented over a regional and continental model domain, which are slightly smaller than North-Rhine Westphalia (NRW) and larger than the pan-European domain (EU), respectively (Figure 1). Additionally, the hydrologic state of the NRW model is corrected with the help of precipitation-radar observations to improve model initialization and the ensuing forecast products. The TMS follows a specific monitoring clock, which is mainly determined by the availability of boundary conditions from operational weather forecasting centers and observation periods. Finally, a number of monitoring products are produced and published online.
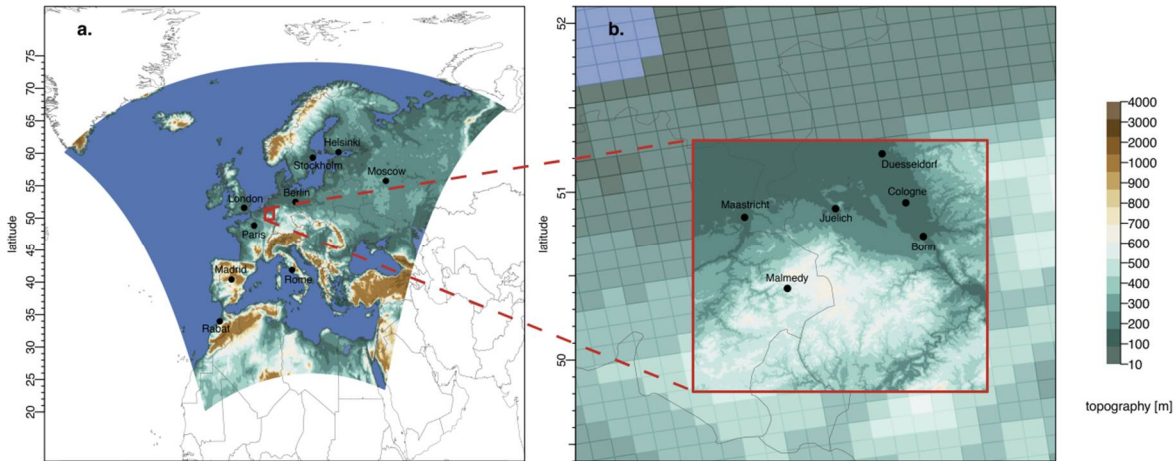
Figure 1. The monitoring domains European (EU, left) and North-Rhine Westphalia (NRW, right). Black circles indicate capitals and major cities of the simulation domains. The domain highlighted in red in the figure on the right is the NRW domain, which is highly equipped with hydrological and hydrometeorological measurement equipment. The resolution differences in (b) illustrate the different grid cell sizes of the model setups, i.e. 12.5km for the EU domain and 500m for the NRW domain.

2.1 Software and hardware components of the Terrestrial Monitoring System, TMS

The dynamic kernel of the TMS is the parallel Terrestrial Systems Modeling Platform (TerrSysMPv1.1.0), which is a scale-consistent, fully integrated groundwater-to-atmosphere model, conserving moisture and energy across all compartments of the geo-ecosystem for different domains. TSMP consists of the numerical weather prediction system (COSMO, v4.21) of the German national weather service (DWD, [24]), the Community Land Model (CLM, v3.5) [25], and the variably saturated surface–subsurface flow code ParFlow (v3.1) [26-28]. The interested reader is referred to the aforementioned publications and [14] for a detailed description of the modeling system. In order to exchange fluxes and states across the individual component models of TSMP and close the terrestrial water and energy cycle, the Ocean-Atmosphere-Sea-Ice-Soil coupler,

OASIS3-MCT [29] is used. The porting, profiling, optimization and scalability of TSMP in a massively parallel supercomputing environment has been documented in [15]. The unique feature of TSMP is that all states and fluxes of the terrestrial water and energy cycle from groundwater across the land surface into the atmosphere are simulated in a mass and energy conservative and scale consistent implementation. Thus, the platform provides simultaneously consistent predictions in all terrestrial compartments, i.e. the subsurface, land surface, and atmosphere.

In the current setup, which has been running continuously since January 2016, the bulk of the monitoring simulations are performed on JURECA, the Jülich Research on Exascale Cluster Architecture. JURECA is a 1872 node (45,216 cores) supercomputer based on T-Platforms V-class server architecture with a peak performance of 1.8 (CPU) + 0.44 (GPU) Petaflops per second. The nodes consist of two 12 core Intel Xeon E5-2680 v3 Haswell CPUs and three different DDR4 memory configurations (128GB, 256GB, 512GB), which are connected through a Mellanox EDR Infiniband network with fat tree topology and a 100GB per second connection to the GPFS storage cluster.

The cluster uses the CentOS 7 Linux distribution as operating system and handles the resource management with the Slurm batch system and Parastation. Also relevant for this work is the fact that cronjobs (tasks scheduled in the background) are prohibited, ssh (secure shell) connections are secured by RSA key-pairs, and compute nodes do not have internet access. This is commonly the case in supercomputing environments, which are not designed and operated for operational use, and must be taken into account in the design of the workflow. The maximum wallclock time is 24 hours and maintenance downtime affects the whole system for several hours on a regular basis (on demand 1-2 per month).

Part of the ensemble simulations of the NRW domain were performed on JUQUEEN, JSCs 5.0 Petaflop IBM Blue Gene/Q supercomputer with 458752 cores and 448TB main memory. JUQUEENs 28 racks are further divided into 32 nodeboards, which are the smallest allocatable units, each consisting of 32 nodes with 16 IBM PowerPC A2 CPU cores (4-way simultaneous multithreading). Each node has 16 GB DDR3 SDRAM and is connected through a 5-D torus (4x4x4x4x2 configuration) network with very high peak bandwidth (40GB s-1). JUQUEENs job submissions are handled by the LoadLeveler job scheduling system. JUQUEEN has been decommissioned in May 2018 and replaced by a new supercomputing architecture, which will be used to generate the ensemble in future.

2.2 Monitoring domain setup

The North-Rhine Westphalia domain

The regional scale domain (Figure 1) covers the south-western part of Germany's North Rhine-Westphalia (NRW) including parts of Belgium, Luxembourg, and the Netherlands. NRW contains the catchments of the rivers Rur, Erft and Swist and partially Rhine, Moselle and Meuse. The domain is 150x150km large and has a convection permitting resolution of 1km for the atmosphere and 0.5km for the land surface and subsurface resulting in a 150x150 and 300x300 grid size with regard to nx and ny, respectively. The number of cells in the vertical dimension is nz=30 for ParFlow, nz=10 for CLM, and nz=50 for COSMO. In the atmospheric model COSMO, the time step size is determined by the spatial discretization and set to dt=10s. Time integration of the relevant exchange fluxes with the land surface and subsurface model CLM and ParFlow is performed by OASIS3-MCT in a 900s interval, which is also the time step size of CLM and ParFlow and the coupling time step between COSMO, CLM and ParFlow. Between 2016 and 2018, the atmospheric initial condition and hourly boundary conditions were provided daily by a deterministic forecasting run of the DWD, uploaded to a FTP server at the Meteorological Institute of the University of Bonn, and then ingested automatically to the TMS every 3h with a maximum lead time of 25h. Note, in May 2018, DWD changed their data policy and provision, which resulted in a hiatus in the boundary condition from the operational forecast. Currently, the NRW monitoring system is adopted to ingest initial and atmospheric boundary information from the 12.5km resolution European monitoring system driven by ECMWF forcing data described below via a one-way nesting every 6 hours and with maximum lead time of 72h. The hydrologic boundary conditions are of the Dirichlet type and

apply a constant pressure head profile. Hydrologic initial conditions are obtained from the previous day's forecast, resulting in a continuous hydrologic time series. Details of the parameterizations and physical parameter values can be found in [14] and [21]. The forecast is distributed over 2 nodes on JURECA and requires approximately 1h compute (wall-clock) time. In a more recent development, the initial conditions are improved continuously via hindsight simulations based on assimilated rain radar information.

In the groundwater-to-atmosphere simulations of the monitoring system, precipitation rates and patterns are always a challenge to model [30]. In weather forecasting, incorrect precipitation fields propagate into the water and energy fluxes of the lower land surface boundary condition that are evapotranspiration and sensible heat, which in turn influence the aforementioned atmospheric processes through two-way feedbacks. However, in the operational setup of the weather services, this error propagation is alleviated via data assimilation, which constantly corrects the atmosphere and land surface states by means of observational data during the assimilation phase of the forecast. In contrast, in the current TMS incorrect precipitation fields are propagated directly into the land surface and groundwater compartments, because of the fully coupled nature of the TMS and the lack of strongly coupled data assimilation capabilities across the different terrestrial compartments, which is still subject of scientific research [31, 32]. In a first correction step for the NRW domain, the precipitation fields from the monitoring run are replaced by rain radar information from high-resolution X-band radar composites at the end of the monitored day. While rain rates from radar observations are also error prone, we expect an overall improvement in comparison to the predicted rain rates from NWP. The observed rain rates in the atmospheric forcing data set are then used to perform an offline subsurface-land surface hydrologic simulation in order to improve the states and fluxes, and, thus, the initial condition for the following day with the observed rain rates. This simulation is called correction run in the following sections.

The rain radar products covering the North-Rhine Westphalia (NRW) domain are provided by the Meteorological Institute, Bonn University. They are composed of the measurements of the polarimetric X-band radar at the Meteorological Institute in Bonn (BoXPol) and the polarimetric X-band radar in Jülich (JuXPol), for technical details of the radar see [33]. The twin-radars provide volume scans consisting of plan position indicators (PPIs) measured at different elevation angles every 5min in order to monitor the 3D structure of precipitating clouds in the North-Rhine Westphalia domain. The rain product is based on the lowest level of the 3D composite and is transferred for ingestion into the monitoring system at the end of each day. For details of the rain product the reader is referred to [34].

The pan-European domain

The continental scale pan-European domain (EU, Figure 1) conforms to the CORDEX EUR-11 standard, which is part of the World Climate Research Program, and covers Europe and parts of northern Africa, western Russia and Asia. The domain is 5450x5300km large and discretized at a resolution of 12.5km resulting in a 436x424 grid size with regard to nx and ny. The number of cells in the vertical direction is nz=15 for ParFlow, nz=10 for CLM, and nz=50 for COSMO, reaching depths and heights of 103m, 3m and about 21km, respectively [19]. The time step size is set to dt = 60s for COSMO and dt = 1h for ParFlow and CLM which is also the coupling frequency. The atmospheric initial conditions and hourly boundary conditions are provided on a daily basis from a high-resolution forecasting run of the European Centre for Medium-Range Weather Forecasts (ECMWF). The hydrologic boundary conditions are of the Dirichlet type and mimic the sea surface with a shallow water table depth along the coastlines [19]. Hydrologic initial conditions are obtained from the previous day's forecast, resulting in a continuous hydrologic time series. Due to potential biases, drifts in hydrologic states and fluxes may occur that have not been diagnosed so far. Details of the parameterizations and physical input parameter values can be found in [19]. A forecast of 72h is performed that is distributed over 6 JURECA nodes and requires approximately 1.5h compute (wall-clock) time.

255   *2.3 Monitoring Clock*

256   Figure 2 shows the monitoring clock i.e. the timeline of the workflows for the NRW and EU
257   domain (Section 3) that is executed automatically on a daily basis. Both workflows are the same
258   except for the precipitation radar correction, which is only applied for NRW, and the provision of
259   the atmospheric initial and boundary condition information, which is provided from the DWD and
260   ECMWF for NRW and EU, respectively. In case of NRW, the monitoring clock starts with the
261   retrieval of the precipitation radar products of the University of Bonn shortly after midnight UTC
262   followed by the correction run of the previous day. This run usually requires less than 1h compute
263   time. DWD's and ECMWF's atmospheric initial and boundary conditions are made available around
264   02:00 UTC and preprocessing starts after the retrieval of the files from a FTP-server. The actual
265   monitoring runs with TSMP commence as soon as the initial and boundary conditions are
266   preprocessed (around 02:15 UTC). The TSMP runs usually require between 1 and 1:30h. In an
267   ensuing step, post-processing is performed and forecasts are made publicly available via videos on
268   YouTube around 03:45 UTC (see Section 3.1). The start of scripts is automatically postponed if
269   required preceding steps are not completed or in case of missing initial and boundary information.
270   The different steps of the monitoring clock are detailed in section 3.
271
272
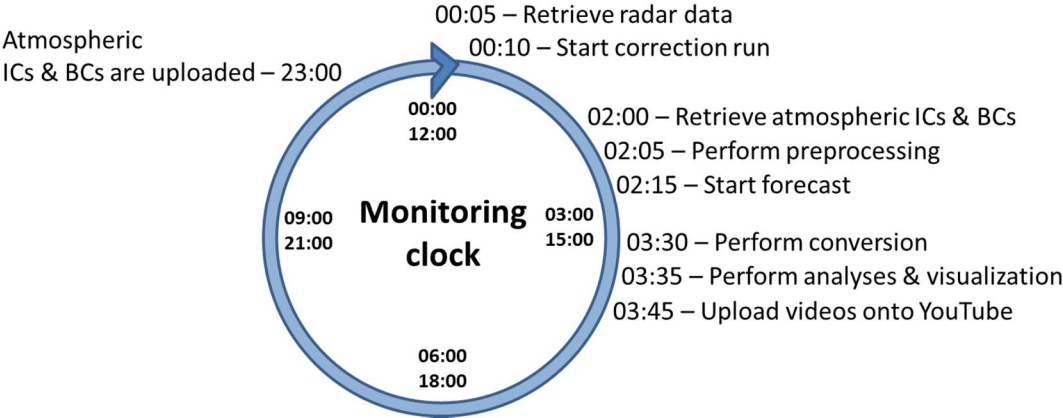
273
274
275   **Figure 2.** Schematic of the monitoring clock for the NRW and EU domain. Note, the rain radar
276   correction is only performed in case of the NRW domain (ICs: Initial conditions; BCs: Boundary
277   conditions).
278

279   **3. Workflows and automation**

280   In this section, the workflow for creating a model run and its technical implementation is
281   described including pre- and post-processing. In addition, the precipitation radar correction
282   approach is outlined in more detail.

283   *3.1 Monitoring EU and NRW*

284   The monitoring workflow for the EU and NRW domains consists of sequentially executed steps
285   detailed below and in Figure 3. Note, both monitoring runs, NRW and EU are based on the same
286   workflow implemented on the supercomputer JURECA of the Jülich Supercomputing Centre. The
287   flowchart in Figure 3 is valid for EU and NRW with some added complexity due to the precipitation
288   radar correction in case of NRW as aforementioned (see Section 3.2 and Figure 4).
289
290
291
292
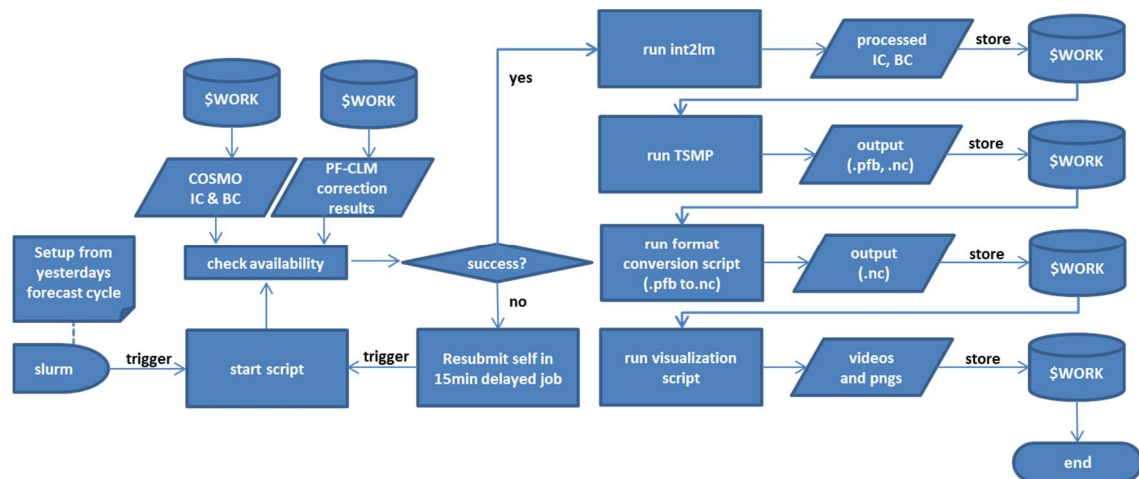
Figure 3. Flowchart for both the EU and NRW monitoring system implemented in the forecast jobscript running on the compute nodes of JURECA, Jülich Supercomputing Centre (JSC). $WORK indicates the execution of the respective workflow step in the working or scratch directory of the HPC environment. Note that both monitoring runs are based on the same workflow.

Retrieval of boundary and initial conditions - All partial differential equation based models require initial and boundary conditions to close the mathematical problem. In TSMP, the hydrologic model ParFlow has fixed boundary conditions of the Neumann and Dirichlet type in case of the EU and NRW domains, and a free overland flow boundary condition at the land surface. Initial conditions are obtained from the previous day's run and from the correction run applying the precipitation radar information in case of NRW. The lateral boundary condition for COSMO is read from a forcing file which was obtained by the nesting approach starting from a global NWP model. These boundary conditions together with the initial condition are provided by DWD (for the NRW domain) and ECMWF (for the CORDEX EUR-11 domain) and downloaded from the corresponding FTP-servers.

Preprocessing - The initial and boundary conditions are obtained from the corresponding global weather prediction systems with a grid spacing of 2.8km and approximately 12km from DWD and ECMWF, respectively. These products are then interpolated to the desired resolution - 1km for NRW and 12.5km for CORDEX EUR-11 - and cropped to the final domain size. Boundary conditions for both domains are created by interpolation. This is done by the standard preprocessing tool int2lm (v. 2.01, [35]) for the COSMO model. The tool interpolates the initial and boundary condition (in Grib or netCDF format) from a coarser source grid and/or larger domain into the desired destination grid. In addition, int2lm renames and transforms all arrays and parameters into a COSMO-readable format, therefore both, DWD data as well as ECMWF data, needs to get preprocessed by int2lm.

Forward simulation - The monitoring system with TSMP is designed to perform continuous, real-time monitoring simulations. Nevertheless, the NWP model COSMO is driven by the aforementioned downloaded and preprocessed initial and boundary conditions and, thus, reinitialized every day. The surface/subsurface models CLM and ParFlow, on the other hand, are restarted with the restart files, which were generated by the previous day's simulation cycle. Due to the slow dynamics in the surface/subsurface, the hydrologic model (i.e. ParFlow-CLM) required an extended spinup simulation with real meteorological forcing prior to the setup of the monitoring system in order to reach a physically consistent dynamic equilibrium. This spinup was performed for both domains in advance to the real-time monitoring and the first monitoring runs were started from these initial conditions. By running the monitoring system continuously, the equilibrium between the subsurface, land surface and atmosphere is maintained and automatically extended. All component models of TSMP have their own set of parameter files, usually called namelists (traditional Fortran nomenclature), that define a large set of runtime information and parameterizations. Input

333   information that is necessary for daily forecast runs, like dates, path to forcing files, run directories
334   or output folders must be consistently set up across all namelists. This is possible in a formalized and
335   consistent manner for the three model components by implementing a setup script environment.
336
337   *Postprocessing and visualization* - The component models of TSMP generate output files in different
338   formats (ParFlow binary, PFB, and netCDF) in hourly intervals. An NCL script (NCAR command
339   language) converts PFB to netCDF and aggregates hourly model output files into one single file for
340   additional post-processing and ensuing archiving. The analyses and visualization are done by a set
341   of Python scripts, which read the output files generated by TSMP with the NetCDF4 Python library
342   in a first step. The output from, for example, ParFlow only consists of pressure and saturation for a
343   given domain. Together with static fields, such as 2D and 3D fields of porosity, specific storage
344   coefficients and slopes in x- and y-direction, the data is then post-processed to the desired analyses,
345   such as surface runoff, groundwater recharge, plant available water, and groundwater table depth.
346   Also standard meteorological products and analyses, such as wind speed, temperature,
347   precipitation, and geopotential heights of pressure levels are generated. After the analysis of output
348   variables is completed, frames for each individual analysis and time step (hourly) are plotted to
349   PNG files with the Python libraries matplotlib and basemap. These PNG files are then rendered with
350   ffmpeg into an AVI-movie.
351
352   *YouTube upload and archiving* - After all previous steps are finished, the generated movies are
353   uploaded via Google API v3 into the corresponding YouTube playlist. Data for the web-app is
354   copied to a webserver and the whole experiment folder is zipped and moved into archive. The raw
355   data is available for at least 10 years.
356
357   Note that the five steps outlined above are contained in three scripts (retrieval of boundary and
358   initial conditions, and preprocessing; forward simulation; and postprocessing and visualization, and
359   YouTube upload and archiving), which are triggered by cronjobs on a different machine over ssh,
360   because user cronjobs are not allowed on JURECA. The data retrieval step and upload/backup step
361   are triggered by separate scripts/cronjobs on the JURECA front nodes and are separated from other
362   steps because the JURECA compute nodes are not connected to the internet. The simulations are set
363   up by a third script/cronjob, which also submits the jobscript to JURECAs job scheduler (slurm) for
364   handling preprocessing, model run and visualization. These scripts contain several reliability
365   mechanisms. For example, delayed scripts restart if download files or checkpoint files are not
366   present, accommodating maintenance downtimes, automatically catching stalled runs and handling
367   jobscripts with 24h lead time in order to optimize job queue position. The overall availability and
368   reliability of the system completely depends on the availability and reliability of the
369   supercomputing resources of JSC. Regular and unplanned system maintenances directly impact the
370   monitoring system and resulting forecast. At this point, no redundancy has been implemented.

371   *3.1 Precipitation radar integration for NRW*

372   As mentioned above and in Section 2, the surface and subsurface models CLM and ParFlow are
373   restarted utilizing the results/restart files of the previous day. This introduces errors due to
374   inaccuracies in the prediction of water fluxes in the groundwater-to-atmosphere system, especially
375   with regard to precipitation. In order to improve the hydrologic states, precipitation radar
376   information is applied in a correction run in an extension of the workflow for NRW. Figure 4 shows
377   the dependencies between the different tasks during the correction run. In a first step, the
378   atmospheric simulation results from previous day's forecast are merged with the rain observations
379   from the radar to generate an atmospheric forcing time series, which is used in an ensuing offline
380   hydrologic simulation with CLM-ParFlow to arrive at the hydrologic initial condition for next day's
381   forecast (Figure 4).
382   *Radar data retrieval and preprocessing* - The radar data is accessible on a server of the Meteorological
383   Institute, Bonn University, and is downloaded shortly after midnight. The radar data are available as

384   netCDF files and are generated every 5 minutes. The grid of the radar data has the same resolution
385   as the forecast run (1km) therefore no interpolation is needed. Because the radar data covers a much
386   larger domain, the data needs to be cropped to the NRW grid sizes. Hourly offline forcing files (i.e.
387   time series of radiation, air temperature, precipitation, wind speeds, barometric pressure and
388   specific humidity at each individual pixel) are generated using the previous monitoring run and
389   observed precipitation from the radar.
390
391   *TSMP correction run and upload/archiving* - TSMP is run in CLM-ParFlow offline mode without
392   COSMO where the newly created forcing files are used as offline atmospheric forcing in CLM. The
393   remainder of the configuration is the same as in the forecasting run. The results are also zipped and
394   moved into the archive.
395
396
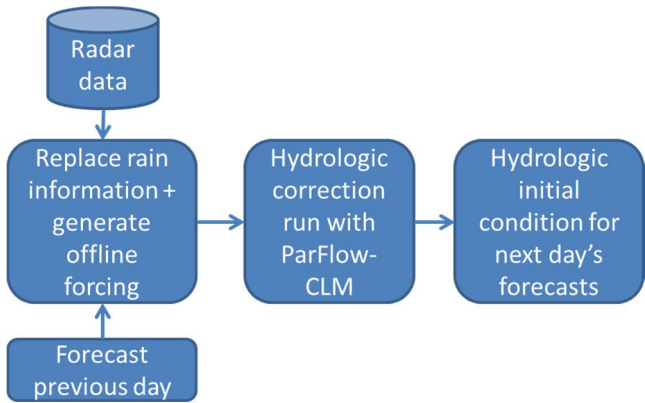
397
398   **Figure 4.** Schematic of the different dependencies between the tasks in the workflow of the
399   correction run.

400   *3.3 Publication of monitoring products*

401   The results are disseminated on the video platform YouTube
402   (https://www.youtube.com/channel/UCGio3ckQwasR5a_kJo1GdOw). Instead of a locally
403   maintained web presence, YouTube is already established and has a strong impact especially
404   beyond the scientific community. It is free and easy to use and has synergies with other social media
405   making it easy to share, link or embed. Additionally, YouTube is fully controllable via a Python API,
406   which is important for the integration into the workflow and automation process presented above.
407   YouTube provides limited but sufficient structuring features for our purposes, which were used to
408   arrange the daily results. The two modeled domains are separated by playlist-sections where every
409   analysis is represented as a playlist and new videos are added automatically. Additionally, we
410   developed a web-app particularly designed for mobile devices that allows displaying meteograms
411   of all analysis products for the current (or a manually selected) location
412   (www.terrsysmp.org/tsmp_app). The raw data is also available via SFTP for the past three months.
413   Note, all data are published in an ad hoc fashion i.e. at this point no quality control has been
414   implemented.

4. Results and discussion

416   Running a fully integrated, groundwater-to-atmosphere terrestrial systems model in forecast
417   mode, opens up new opportunities. In addition to weather variables, special emphasis on the
418   analyses of hydrologic variables enables new applications that are unique so far. For example,
419   forecasted analyses of plant available water is useful for agricultural applications, surface runoff for
420   flood forecasting and hydropower, and groundwater recharge, water table depth and water column
421   storage for water resources management and drought prediction. In the following sections, example
422   results of the different monitoring experiments are shown.

423

4.1 Monitoring EURO CORDEX and NRW

In comparison to widely available meteorological forecasts, the unique feature of the monitoring system are experimental analyses and monitoring products of all state variables and fluxes from groundwater across the land surface into the atmosphere. A large number of variables can be accessed at https://www.youtube.com/channel/UCGio3ckQwasR5a_kJo1GdOw. Below, some examples are shown for more classical atmospheric products (Figure 5 and 6), a hydrologic variable (Figure 7) over Europe during the heat wave of 2018, and hydrologic variables over NRW (Figure 8 and 9) during the flooding in January 2018, which are not commonly available. For example, Figure 9 shows groundwater recharge, which is a variable of great interest to public water managers and agriculture.

Figure 5 shows the 2m air temperature forecasts over Europe on August 7th, which was the peak of the heat wave in Germany in 2018. Temperatures above 35 ᵒC were recorded in Germany during that time period. In addition, meteograms are provided for the location of the city of Jülich, Germany, for 2m air temperature, sea level barometric pressure, 2m specific humidity, 20m wind speed, and precipitation. Figure 6 shows the precipitation forecast over Europe including precipitation meteograms for a number of European capitals. Both figures constitute standard NWP-type products. Figure 7 shows the forecasted change in plant available soil water as a new product, which is the change in the amount of water that is available to plants via root water uptake at a matric potential > 10m. The figure illustrates the overall recession of plant available water on the order of -10mm over a period of 72h with localized recharge due to local precipitation events toward the end of the forecast period.

445

446
447
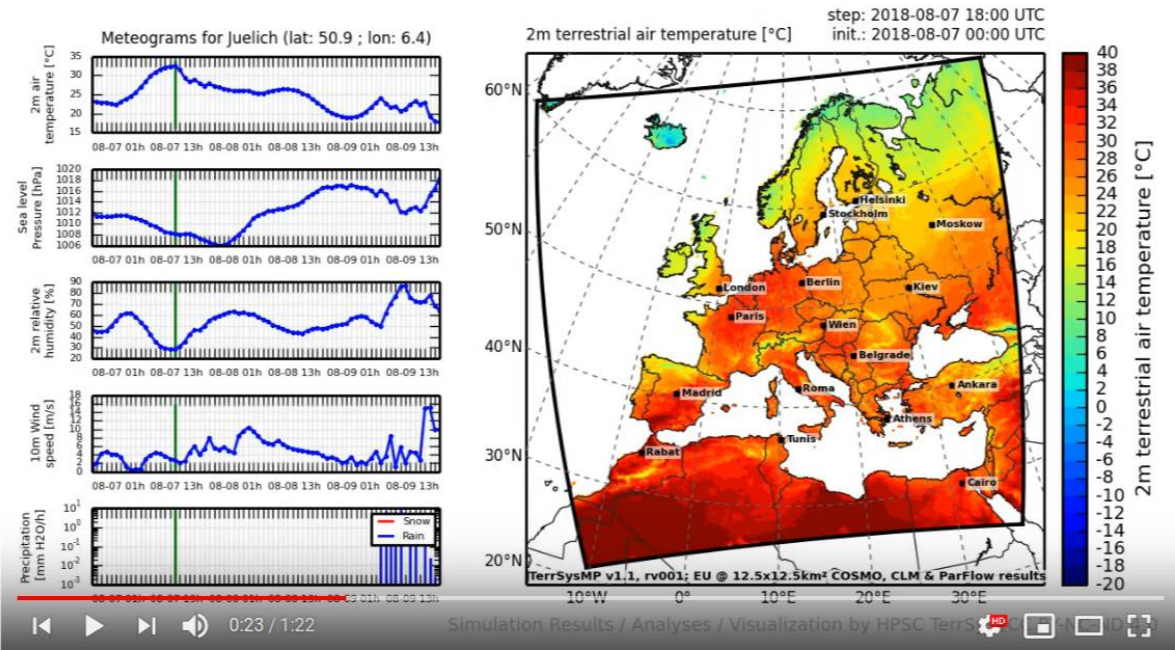
Figure 5. Monitoring output of TSMP (CORDEX EUR-11 domain) for the terrestrial 2m air temperature [°C] at the peak of the heat wave on August 7th, 2018. On the left from top to bottom, the meteograms depict 2m air temperature [°C], sea level pressure [hPa], 10m wind speed [ms 1], and precipitation [mmh-1] in Jülich (latitute:50.9, longitude: 6.4), Germany.

452
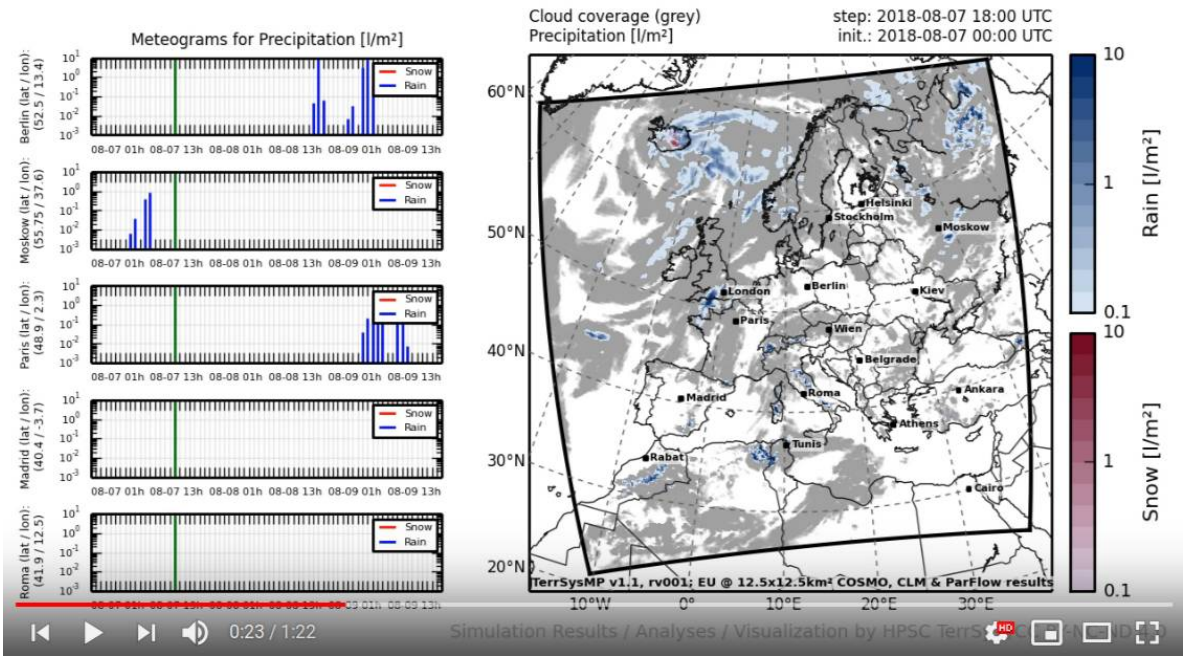
Figure 6. Monitoring output of TSMP (CORDEX EUR-11 domain) for precipitation [lm⁻² or mm] in logarithmic scale on August 7th, 2018. On the left from top to bottom, the meteograms depict precipitation rates (snow and rain) [lm⁻² or mm] for the European capitals Berlin, Moscow, Paris, Madrid and Rome.
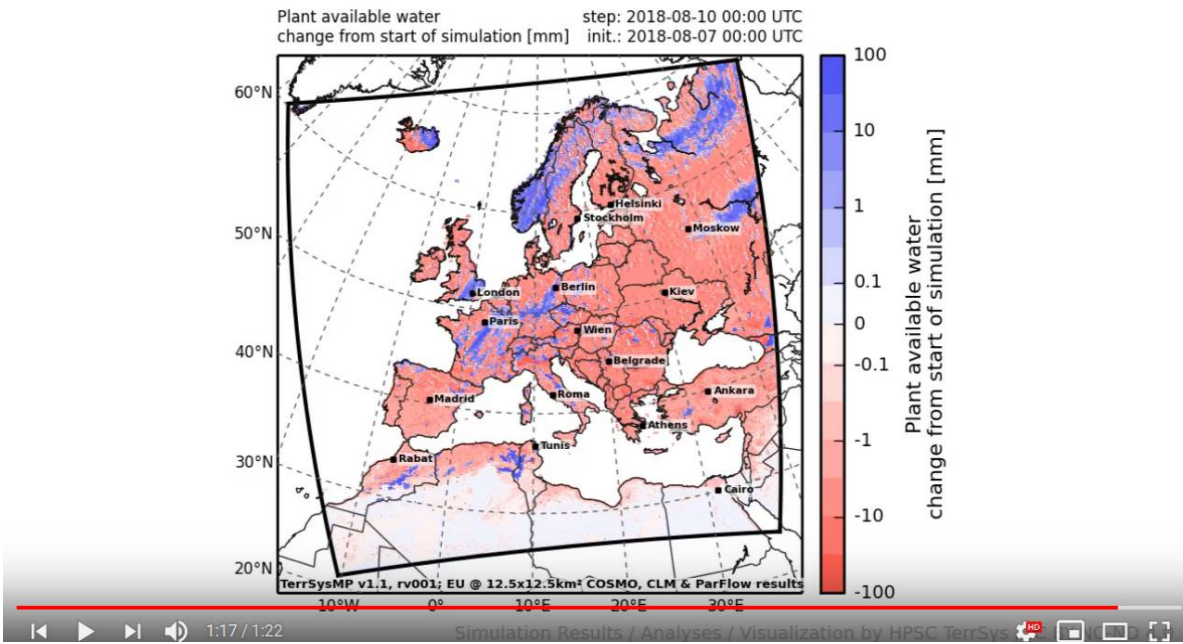
Figure 7. Monitoring output of TSMP (CORDEX EUR-11 domain) of the change of plant available water [mm] over the course of the prediction period of 72h (between August 7 and August 10, 2018).

Figure 8 shows the forecasted change in groundwater table depth over the prediction period of 24h (8th of January, 2018) over the NRW domain. The forecast suggests widespread recession of groundwater (positive values) with increasing groundwater table depth and localized decreases in water table depth in recharge areas. This is in contrast to the flooding of the Rhine River during the same period, which was mainly caused by heavy precipitation and snow melt in Southern Germany

471   and the Alps. The predicted groundwater recharge shown in Figure 9 is spatially quite
472   heterogeneous contradicting the common assumption of spatially uniform recharge areas along
473   topographic ridges and heights. Especially in the Eifel region in the south of the monitoring domain,
474   recharge areas alternate with discharge areas over small distances, which is difficult to simulate with
475   simplified modeling approaches separating the groundwater compartment from the soil zone and
476   land surface.
477
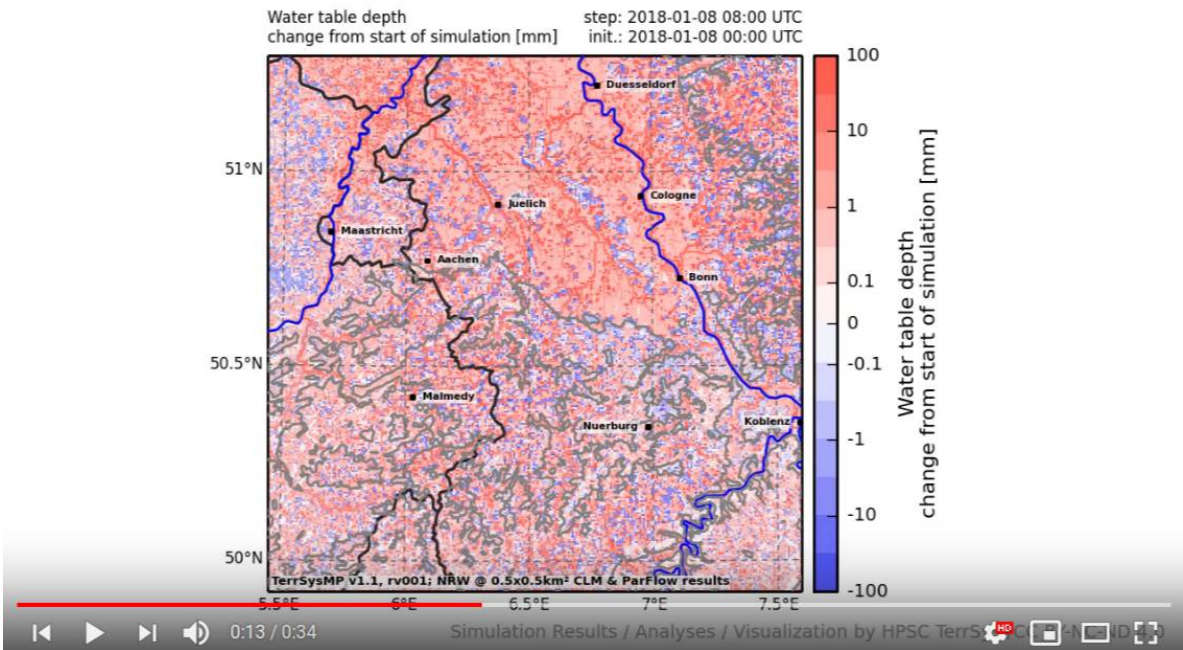
478
479
480   **Figure 8.** Monitoring output of TSMP (NRW) for the water table depth change [mm] in
481   logarithmic scale. The change is estimated relative to the initial condition at the beginning of the
482   monitoring run. Negative values indicate a rise of the water table.
483
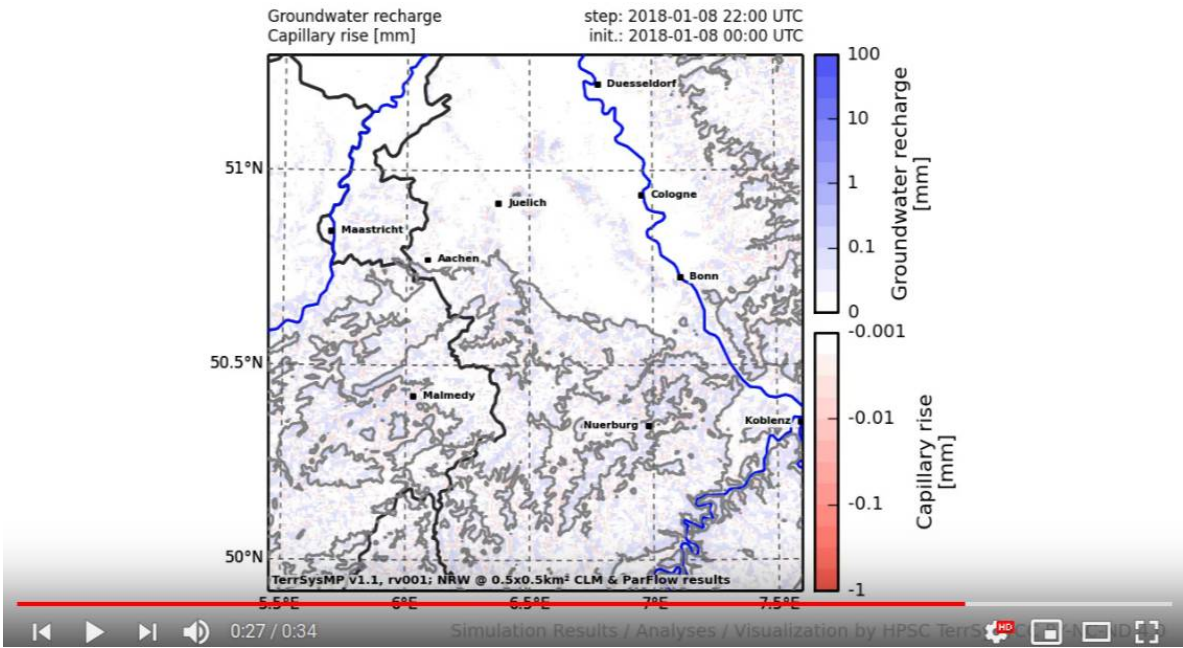
484
485
486   **Figure 9.** Monitoring output of TSMP (NRW) for groundwater recharge (positive) and capillary
487   rise (negative) [mm] i.e. the plant available water storage change [mm (sym log)]. The change is
488   relative to the initial condition. The plant available water is the water that is stored in the pore space
489   at a matric potential larger than -10m.

490

491   *4.2 Radar correction for NRW*

492   Figures 10 to 12 show the impact of the rain radar correction on the hydrology using the
493 precipitation radar information as forcing in January 2018. Figure 10 shows the cumulative
494 precipitation fields from the monitoring and correction run (small panels on the right), and the
495 difference between both runs. One can clearly distinguish regions of over- and underestimation of
496 precipitation, which results in correlated differences in air temperature (Figure 11) and, more
497 pronounced, in surface runoff (Figure 12). While precipitation products from radars are error prone,
498 we expect an improvement in the simulated states especially with regard to their spatial
499 distribution.

500

501
502
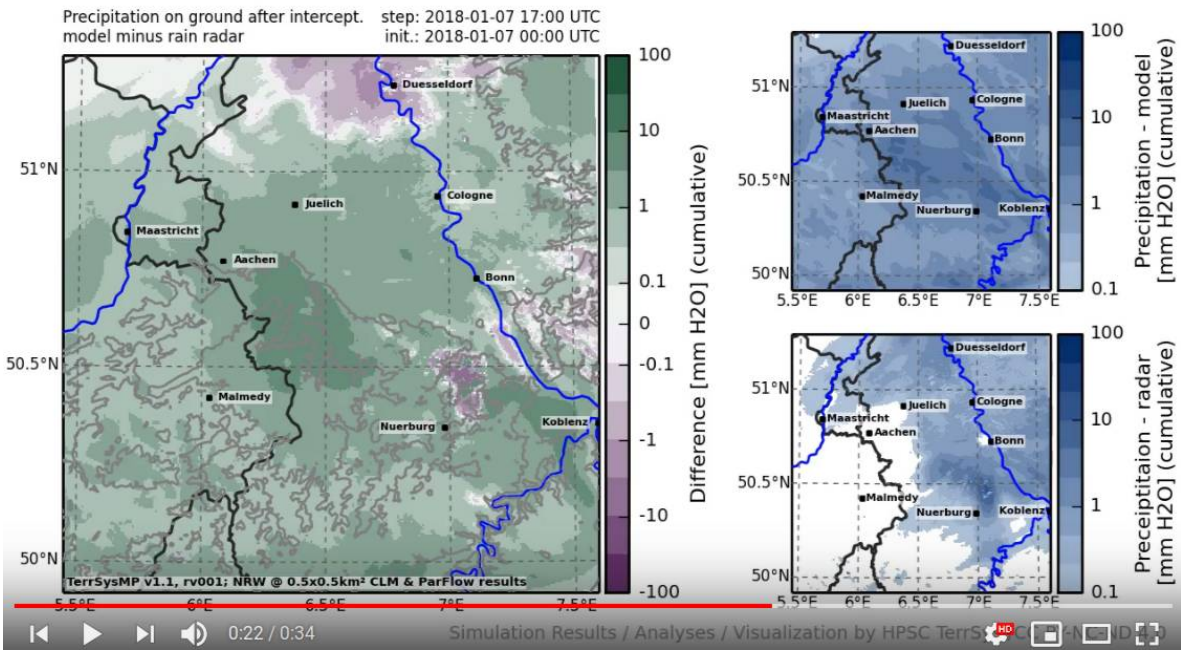
503   **Figure 10.** Difference plot for precipitation [mm] between simulated and radar precipitation
504 (left). The panels on the right show the simulated precipitation (top) and radar-estimated
505 precipitation (bottom).

506
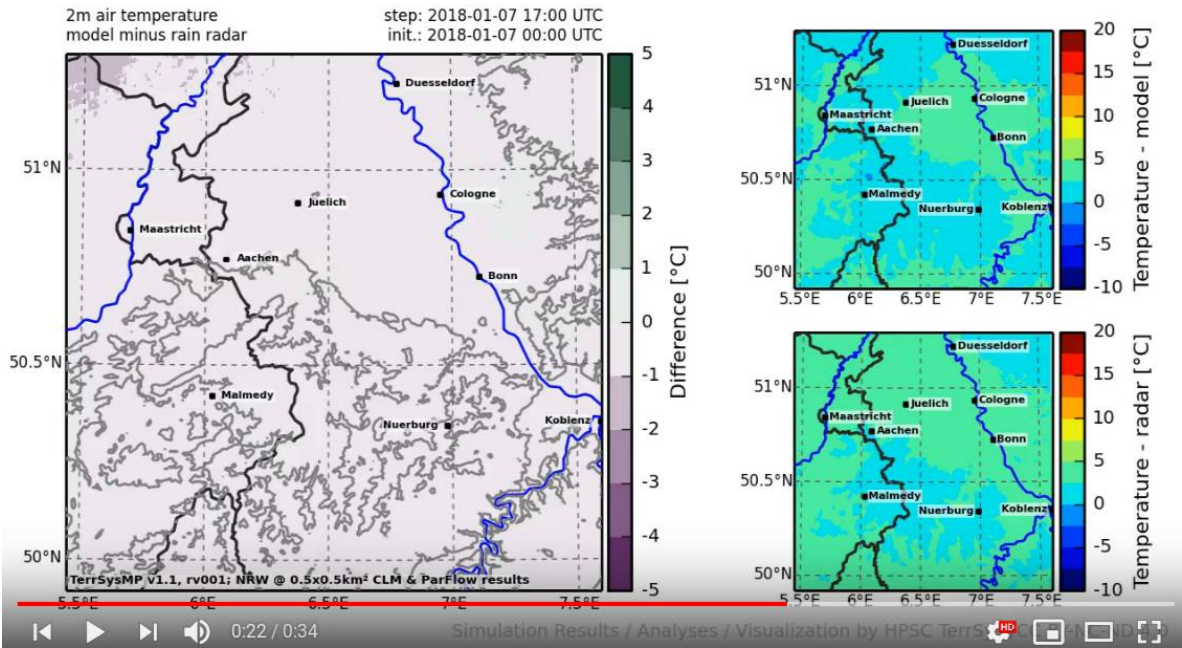
Figure 11. Difference plot for 2m air temperature [oC] between uncorrected and precipitation radar corrected simulations. The panels on the right show the temperatures from the uncorrected (top) and precipitation radar corrected simulations (bottom).
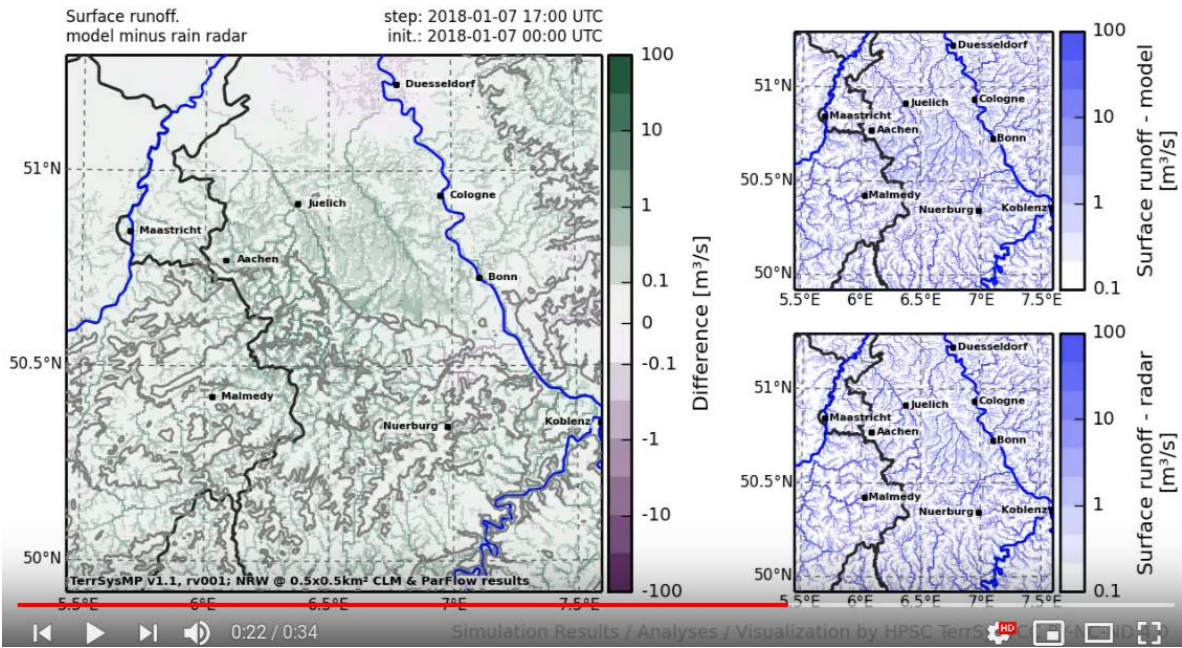
Figure 12. Difference plot for surface runoff [m3s-1] between uncorrected and precipitation radar corrected simulations. The panels on the right show the runoff from the uncorrected (top) and precipitation radar corrected simulations (bottom).

5. Summary and conclusions

We presented a real-time terrestrial monitoring system (TMS) that closes the water and energy cycles from the groundwater into the atmosphere. The system provides forecasts of all states and fluxes of the water and energy cycle and a physically consistent digital image of the terrestrial system. The TMS has been implemented over a European continental domain (EU) and a regional domain covering parts of North Rhine Westphalia and bordering countries (NRW). In case of NRW,

a correction of the hydrologic states is achieved by ingesting precipitation radar information into the monitoring system in an offline correction run, in order to improve the initialization of the land component of the ensuing monitoring run. The terrestrial monitoring system is experimental and still requires comprehensive validation, which is subject of ongoing research. The system gained some attention in the community and beyond. For example, the videos were watched more than 26,000 times since the commencement in January 2016. There is great potential in extending the monitoring to e.g. the seasonal time scale, adding data assimilation for improved model initialization, and the development of monitoring products for industry and public sectors. The complete runtime system and output is provided freely via sftp (for access contact corresponding author).

Author Contributions: Conceptualization, S.K., C.S. and K.G.; methodology, S.K., C.S. and K.G.; software, V.K. and F.G..; formal analysis, S.K., F.G., K.G.; investigation, S.K., F.G., K.G.; data curation, F.G.; writing—original draft preparation, F.G., S.K.; writing—review and editing, S.K., F.G., S.B., K.G., H.-J. H.-F., J.K., W.K., V.K., F.P., S.P., S.T, P.S., C.S., M.S.; visualization, F.G., K.G., S.B.; supervision, S.K.; project administration, S.K.; funding acquisition, S.K., C.S.

Funding: This research work was supported by the SFB/TR32 Patterns in Soil-Vegetation-Atmosphere Systems: Monitoring, Modeling and Data Assimilation project funded by the Deutsche Forschungsgemeinschaft (DFG) and TERENO.

Acknowledgments: The authors gratefully acknowledge the computing time granted through the Board of Directors on the supercomputer JURECA and JQUEEN at Forschungszentrum Jülich. We gratefully acknowledge the provision of the atmospheric boundary data by the European Centre for Medium-range Weather Forecasting and the German Weather Service.

Conflicts of Interest: The authors declare no conflict of interest.

References

1. Swinbank, R., Kyouda, M., Buchanan, P., Froude, L., Hamill, T.M., Hewson, T.D., Keller, J.H., Matsueda, M., Methven, J., Pappenberger, F., Scheuerer, M., Titley, H.A., Wilson, L., Yamaguchi, M. The TIGGE Project and Its Achievements. *Bull. Amer. Meteor. Soc.* **2015**, 97, 49–67. https://doi.org/10.1175/BAMS-D-13-00191.1

2. Damrath, U., Doms, G., Frühwald, D., Heise, E., Richter, B., Steppeler, J. Operational quantitative precipitation forecasting at the German Weather Service. *J. Hydrol.* **2000**, 239, 260–285. https://doi.org/10.1016/S0022-1694(00)00353-X

3. Palmer, T. The ECMWF Ensemble Prediction System: Looking Back (more than) 25 Years and Projecting Forward 25 Years. **2018**. arXiv:1803.06940 [physics]

4. Lynch, P. The origins of computer weather prediction and climate modeling. *J. Comp. Phys.*, **2008**, Predicting weather, climate and extreme events 227, 3431–3444. https://doi.org/10.1016/j.jcp.2007.02.034

5. Bauer, P., Thorpe, A., Brunet, G. The quiet revolution of numerical weather prediction. *Nature* **2015**, 525, 47–55. https://doi.org/10.1038/nature14956

6. Saha, S., Moorthi, S., Wu, X., Wang, J., Nadiga, S., Tripp, P., Behringer, D., Hou, Y.-T., Chuang, H., Iredell, M., Ek, M., Meng, J., Yang, R., Mendez, M.P., van den Dool, H., Zhang, Q., Wang, W., Chen, M., Becker, E. The NCEP Climate Forecast System Version 2. *J. Climate* **2013**, 27, 2185–2208. https://doi.org/10.1175/JCLI-D-12-00823.1

7. Roebber, P.J., Schultz, D.M., Colle, B.A., Stensrud, D.J. Toward Improved Prediction: High-Resolution and Ensemble Modeling Systems in Operations. *Wea. Forecasting* **2004**, 19, 936–949. https://doi.org/10.1175/1520-0434(2004)019<0936:TIPHAE>2.0.CO;2

8. Roo, A.P.J. de, Gouweleeuw, B., Thielen, J., Bartholmes, J., Bongioannini-Cerlini, P., Todini, E., Bates, P.D., Horritt, M., Hunter, N., Beven, K., Pappenberger, F., Heise, E., Rivin, G., Hils, M., Hollingsworth, A., Holst, B., Kwadijk, J., Reggiani, P., Dijk, M.V., Sattler, K., Sprokkeref, E. Development of a European flood forecasting system. *Intern. J. River Basin Management* **2003**, 1, 49–59. https://doi.org/10.1080/15715124.2003.9635192

9. Thielen, J., Bartholmes, J., Ramos, M.-H., de Roo, A. The European Flood Alert System – Part 1: Concept and development. *Hydrol. Earth Syst. Sci.* **2009**, 13, 125–140. https://doi.org/10.5194/hess-13-125-2009

575 10. Refsgaard, J.C. Validation and Intercomparison of Different Updating Procedures for Real-Time
576   Forecasting. *Hydrol. Res.* **1997**, 28, 65–84. https://doi.org/10.2166/nh.1997.0005

577 11. Emerton, R., Zsoter, E., Arnal, L., Cloke, H.L., Muraro, D., Prudhomme, C., Stephens, E.M., Salamon, P.,
578   Pappenberger, F. Developing a global operational seasonal hydro-meteorological forecasting system:
579   GloFAS-Seasonal v1.0. *Geosci. Model Dev.* **2018**, 11, 3327–3346. https://doi.org/10.5194/gmd-11-3327-2018

580 12. Shukla, S., McNally, A., Husak, G., Funk, C. A seasonal agricultural drought forecast system for
581   food-insecure   regions   of   East   Africa.   *Hydrol.   Earth   Syst.   Sci.*   **2014**,   18,   3907–3921.
582   https://doi.org/10.5194/hess-18-3907-2014

583 13. De Lange, W.J., Prinsen, G.F., Hoogewoud, J.C., Veldhuizen, A.A., Verkaik, J., Oude Essink, G.H.P., van
584   Walsum, P.E.V., Delsman, J.R., Hunink, J.C., Massop, H.T.L., Kroon, T. An operational, multi-scale,
585   multi-model system for consensus-based, integrated water management and policy analysis: The
586   Netherlands   Hydrological   Instrument.   *Env.   Mod.   &   Soft.*   **2014**,   59,   98–108.
587   https://doi.org/10.1016/j.envsoft.2014.05.009

588 14. Shrestha, P., Sulis, M., Masbou, M., Kollet, S., Simmer, C. A Scale-Consistent Terrestrial Systems Modeling
589   Platform Based on COSMO, CLM, and ParFlow. *Mon. Wea. Rev.* **2014**, 142, 3466–3483.
590   https://doi.org/10.1175/MWR-D-14-00029.1

591 15. Gasper, F., Goergen, K., Shrestha, P., Sulis, M., Rihani, J., Geimer, M., Kollet, S. Implementation and
592   scaling of the fully coupled Terrestrial Systems Modeling Platform (TerrSysMP v1.0) in a massively
593   parallel supercomputing environment – a case study on JUQUEEN (IBM Blue Gene/Q). *Geosci. Mod. Dev.*
594   **2014** 7, 2531–2543. https://doi.org/10.5194/gmd-7-2531-2014

595 16. Simmer, C., I. Thiele-Eich, M. Masbou, W. Amelung, S. Crewell, B. Diekkrueger, F. Ewert, H.-J. Hendricks
596   Franssen, A. J. Huisman, A. Kemna, N. Klitzsch; S. Kollet, M. Langensiepen, U. Loehnert, M. Rahman, U.
597   Rascher, K. Schneider, J. Schween, Y. Shao, P. Shrestha, M. Stiebler, M. Sulis, J. Vanderborght, H.
598   Vereecken, J. van der Kruk, T. Zerenner, and G. Waldhoff. Monitoring and Modeling the Terrestrial
599   System from Pores to Catchments - the Transregional Collaborative Research Center on Patterns in the
600   Soil-Vegetation-Atmosphere   System.   *Bull.   Am.   Meteorol.   Soc.*   **2014**,   96,   1765–1787.   doi:
601   http://dx.doi.org/10.1175/BAMS-D-13-00134.1

602 17. Rahman, M., Sulis, M., Kollet, S.J. The concept of dual-boundary forcing in land surface-subsurface
603   interactions of the terrestrial hydrologic and energy cycles. *Wat. Resour. Res.* **2014**, 50, 8531–8548.
604   https://doi.org/10.1002/2014WR015738

605 18. Rahman, M., M. Sulis, and S.J. Kollet. The subsurface-land surface-atmosphere connection under
606   convective conditions, *Adv. in Water Resour.* **2015**, 83, 240-249.

607 19. Keune, J., F. Gasper, K. Goergen, A. Hense, P. Shrestha, M. Sulis, and S. Kollet. Studying the influence of
608   groundwater representations on land surface-atmosphere feedbacks during the European heat wave in
609   2003,   J.   *Geophys.   Res.   Atmos.*   **2016**,   121,   13,   301–13,325,   doi:10.1002/2016JD025426.
610   doi:10.1002/2016JD025426.

611 20. Sulis, M., Williams, J.L., Shrestha, P., Diederich, M., Simmer, C., Kollet, S.J., Maxwell, R.M. Coupling
612   Groundwater, Vegetation, and Atmospheric Processes: A Comparison of Two Integrated Models. *J.*
613   *Hydrometeor.* **2017**, 18, 1489–1511. https://doi.org/10.1175/JHM-D-16-0159.1

614 21. Sulis, M., J. Keune, P. Shrestha, C. Simmer, and S. J. Kollet. Quantifying the Impact of Subsurface-Land
615   Surface Physical Processes on the Predictive Skill of Subseasonal Mesoscale Atmospheric Simulations. *J.*
616   *Geophys. Res. Atmos.* **2018**, 123(17), 9131-9151, DOI: 10.1029/2017JD028187.

617 22. Keune, J., Sulis, M., Kollet, S., Siebert, S., Wada, Y. Human Water Use Impacts on the Strength of the
618   Continental   Sink   for   Atmospheric   Water.   *Geophys.   Res.   Let.*   **2018**,   45,   4068–4076.
619   https://doi.org/10.1029/2018GL077621

620 23. Keune, J., Sulis, M., Kollet, S., Potential added value of incorporating human water use in the simulation of
621   evapotranspiration and precipitation in a continental-scale bedrock-to-atmosphere modeling system. *J.*
622   *Adv. Modeling Earth Sys.* (under review)

623 24. Baldauf, M., Seifert, A., Förstner, J., Majewski, D., Raschendorfer, M., Reinhardt, T. Operational
624   Convective-Scale Numerical Weather Prediction with the COSMO Model: Description and Sensitivities.
625   *Mon. Wea. Rev.* **2011**, 139, 3887–3905. https://doi.org/10.1175/MWR-D-10-05013.1

626 25. Oleson, K.W., Niu, G.-Y., Yang, Z.-L., Lawrence, D.M., Thornton, P.E., Lawrence, P.J., Stöckli, R.,
627   Dickinson, R.E., Bonan, G.B., Levis, S., Dai, A., Qian, T. Improvements to the Community Land Model and

628 their impact on the hydrological cycle. *J. Geophys. Res: Biogeosci* **2008**, 113.
629 https://doi.org/10.1029/2007JG000563

630 26. Jones, J.E., Woodward, C.S. Newton–Krylov-multigrid solvers for large-scale, highly heterogeneous,
631 variably saturated flow problems. *Adv. Water Resour.* **2001**, 24, 763–774.
632 https://doi.org/10.1016/S0309-1708(00)00075-0

633 27. Kollet, S.J., Maxwell, R.M., 2006. Integrated surface–groundwater flow modeling: A free-surface overland
634 flow boundary condition in a parallel groundwater flow model. Advances in Water Resources 29, 945–958.
635 https://doi.org/10.1016/j.advwatres.2005.08.006

636 28. Maxwell, R.M. A terrain-following grid transform and preconditioner for parallel, large-scale, integrated
637 hydrologic modeling. *Adv. Water Resour.* **2013**, 53, 109–117. https://doi.org/10.1016/j.advwatres.2012.10.001

638 29. Valcke, S. The OASIS3 coupler: a European climate modelling community software. *Geosci. Model Dev.*
639 **2013**, 6, 373–388. https://doi.org/10.5194/gmd-6-373-2013

640 30. Rodwell, M.J., Magnusson, L., Bauer, P., Bechtold, P., Bonavita, M., Cardinali, C., Diamantakis, M.,
641 Earnshaw, P., Garcia-Mendez, A., Isaksen, L., Källén, E., Klocke, D., Lopez, P., McNally, T., Persson, A.,
642 Prates, F., Wedi, N. Characteristics of Occasional Poor Medium-Range Weather Forecasts for Europe. *Bull.*
643 *Amer. Meteor. Soc.* **2013**, 94, 1393–1405. https://doi.org/10.1175/BAMS-D-12-00099.1

644 31. Kurtz, W., He, G., Kollet, S. J., Maxwell, R. M., Vereecken, H., and Hendricks Franssen, H.-J. TerrSysMP–
645 PDAF (version 1.0): a modular high-performance data assimilation framework for an integrated land
646 surface–subsurface model. *Geosci. Model Dev.* **2016**, 9, 1341-1360, doi:10.5194/gmd-9-1341-2016.

647 32. Zhang, H., Kurtz, W, Kollet, S., Vereecken, H. Hendricks Franssen, H.J. Comparison of different
648 assimilation methodologies of groundwater levels to improve predictions of root zone soil moisture with
649 an integrated terrestrial systems model. *Adv. Water Resour.* **2018**, 111, 224-238.

650 33. Diederich, M., A. Ryzhkov, C. Simmer, P. Zhang, and S. Troemel. Use of specific attenuation for rainfall
651 measurement at X-band radar wavelengths - Part 1: Radar calibration and partial beam blockage
652 estimation. *J. Hydrometeor.* **2015**, 16(2), 487-502, https://doi.org/10.1175/JHM-D-14-0066.1

653 34. Diederich, M., Ryzhkov, A., Simmer, C., Zhang, P., Trömel, S. Use of Specific Attenuation for Rainfall
654 Measurement at X-Band Radar Wavelengths. Part II: Rainfall Estimates and Comparison with Rain
655 Gauges. *J. Hydrometeor.* **2015**, 16(2), 503–516. https://doi.org/10.1175/JHM-D-14-0067.1

656 35. Schättler, U. and U. Blahak, A Description of the Nonhydrostatic Regional COSMO-Model Part V:
657 Preprocessing: Initial and Boundary Data for the COSMO-Model. 2018. Available online:
658 http://www.cosmo-model.org/content/model/documentation/core/int2lm_2.03.pdf (accessed on
659 23.10.2018).